

Benzimidazole Derivatives: Selective Fluorescent Chemosensors for the Picogram Detection of Picric Acid

Jin-Feng Xiong,^{†,§} Jian-Xiao Li,^{⊥,§} Guang-Zhen Mo,[†] Jing-Pei Huo,[⊥] Jin-Yan Liu,[†] Xiao-Yun Chen,^{*,‡} and Zhao-Yang Wang^{*,†,||}

[†]School of Chemistry and Environment, South China Normal University, Guangzhou, 510006, P. R. China

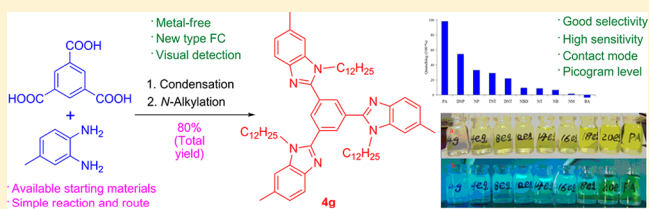
^{||}Key Laboratory of Theoretical Chemistry of Environment, Ministry of Education, Guangzhou, 510006, P. R. China

[⊥]School of Chemistry and Chemical Engineering, South China University of Technology, Guangzhou, 510640, P. R. China

[‡]Institute of Organic Chemistry, RWTH Aachen University, Landoltweg 1, D-52074 Aachen, Germany

Supporting Information

ABSTRACT: 1,3,5-Tri(1*H*-benzo[*d*]imidazol-2-yl)benzene derivatives, as a new kind of fluorescent chemosensor for the detection of nitroaromatic explosives, are designed and synthesized by simple N-hydrocarbylation. Among 16 obtained compounds, compound **4g** has the best capability for detection of picric acid (PA), having good selectivity and high sensitivity. The detection of PA with **4g** solution-coated paper strips at the picogram level is developed. A simple, portable, and low-cost method is provided for detecting PA in solution and contact mode.



1. INTRODUCTION

Recently, great research interest has been attracted to the development of new efficient fluorescence quenching methods for the detection of nitroaromatic explosives,^{1–7} especially for picric acid (PA).^{8–18} However, there are only a few reports about fluorescent chemosensors (FCs) with good selectivity and high sensitivity for PA based on small molecule organic compounds without ion-assisted fluorescence enhancement.^{19–24} From the viewpoint of structure type, these small molecule organic FCs for PA are mainly linear^{19,21,22,24} or planar^{20,23} benzoaromatic derivatives (Scheme 1). Usually their synthesis may suffer from certain limitations, such as a lengthy synthetic route,^{19–21} a low total yield of the target molecule,^{19,22–24} uncommon starting materials,^{20,23} and the need for expensive Pd catalyst.^{19,20,22,23}

In addition, it is well-known that long-range energy transfer as a fluorescence quenching mechanism usually has better sensitivity compared to short-range charge transfer,^{22,23,25} and unfortunately the latter has been reported for most small molecule organic FCs for PA at present.^{19–21,24} Moreover, the solid-state detection of PA has earned much attention due to its simplicity.^{19–23} Thus, a new small molecule organic FC for PA with good selectivity, high sensitivity, and practical application in solid-state trace detection at the picogram level by the long-range energy transfer mechanism is becoming attractive.

Due to easy access to benzimidazole derivatives, they have been widely used in many fields, such as biomedicine,^{26–29} liquid materials,^{30–32} flame retardants,³³ supramolecular chemistry,³⁴ coordination chemistry,³⁵ and CO₂ chemosensors.³⁶ However, to the best of our knowledge, there is no

report about the use of benzimidazole derivatives as FCs for PA detection.

Herein, on the basis of our previous research on nitrogen-containing heterocyclic compounds,^{29,32,37–39} a new kind of FC based on 1,3,5-tri(1*H*-benzo[*d*]imidazol-2-yl)benzene (TBB, Scheme 1) for detecting nitroaromatic explosives is designed and synthesized by a simple route using very readily available starting materials (Schemes 2 and 3). Fortunately, this benzimidazole-type FC **4g** (Scheme 1) with good selectivity and high sensitivity not only can detect PA in solution but can also be used in the contact mode for PA trace detection at the picogram level.

2. RESULTS AND DISCUSSION

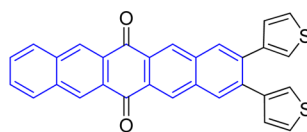
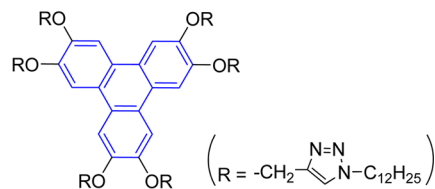
2.1. Design and Synthesis of Target Molecules 3–6.

To investigate the influences of alkyl chain length, side-chain saturation, and triazole modification on fluorescence quenching, the target molecules 3–6 are designed and synthesized. There are three benzimidazole moieties with very strong fluorescence in these 1,3,5-tri(1*H*-benzo[*d*]imidazol-2-yl)benzene (TBB) derivatives. Simultaneously, because the solubility of functional molecules in common organic solvents will be improved and the intermolecular excimer formation through π – π interaction will be prevented in the presence of long-chain alkyl groups, various N-alkylated benzimidazoles are synthesized by condensation and subsequent N-hydrocarbylation using readily available *o*-phenylenediamines **1**, trimesic acid **2**, and bromohydrocarbons as starting materials (Scheme 2).

Received: October 6, 2014

Published: November 11, 2014

Scheme 1. Representative FCs with Good Selectivity and High Sensitivity for PA Based on Small Molecule Organic Compounds without Ion-Assisted Fluorescence Enhancement

 Typical linear benzoaromatic derivative:²²

 Typical planar benzoaromatic derivative:²³

This work:

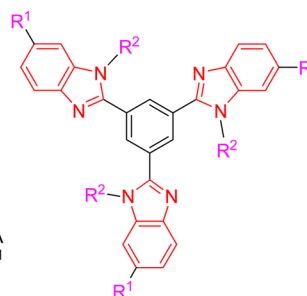
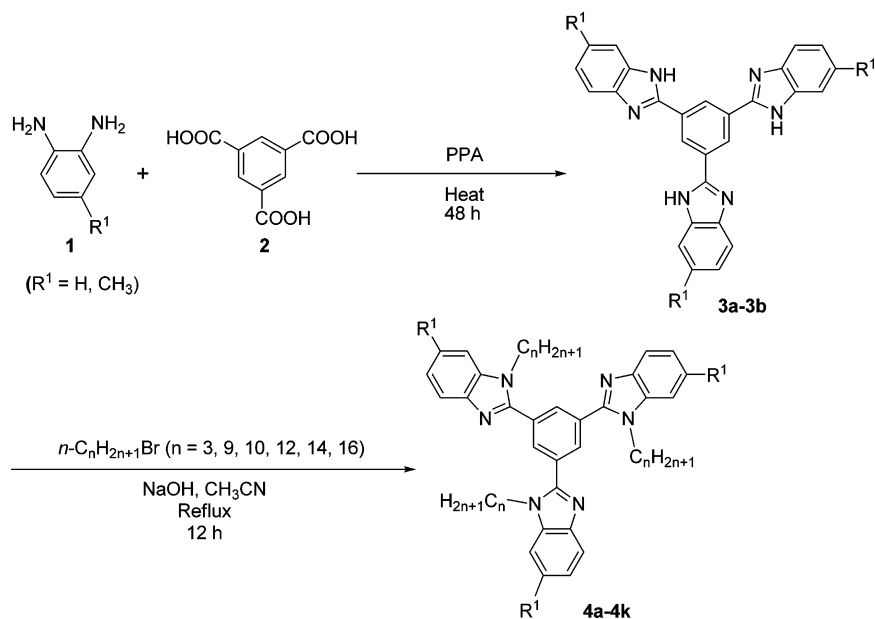
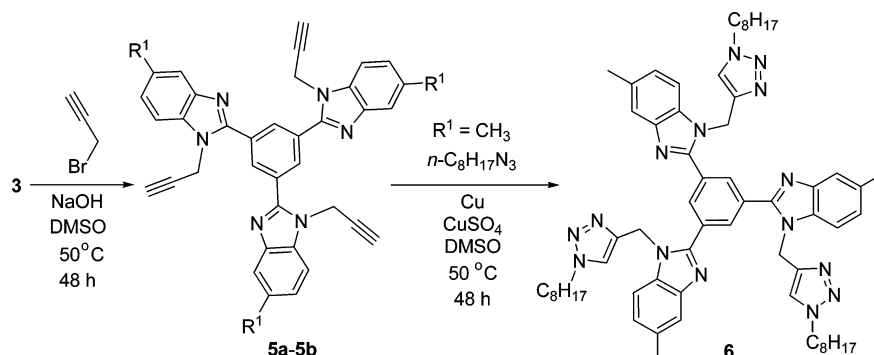
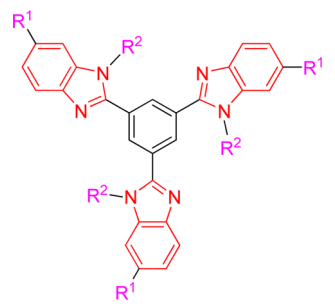
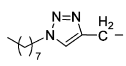
 Benzimidazole derivatives as a new type PA fluorescent chemosensor (for compound **4g**, R¹ = CH₃, R² = *n*-C₁₂H₂₅)

Scheme 2. Synthesis of TBB Derivatives 3a,b and 4a–k

Scheme 3. Synthesis of TBB Derivatives 5a,b and 6


Table 1. Yields, λ_{\max} and λ_{em} of the TBB Compounds 3–6


Entry	Compound	R ¹	R ²	Yield (%)	λ_{\max} (nm) ^a	λ_{em} (nm) ^a	Stoke's shift (nm)
1 ^b	3a	H	H	81	316.0	379.1	63.1
2	3b	CH ₃	H	82	322.8	386.5	63.7
3	4a	H	<i>n</i> -C ₃ H ₇ -	61	301.5	381.0	79.5
4	4b	H	<i>n</i> -C ₉ H ₁₉ -	91	300.0	361.1	61.1
5	4c	CH ₃	<i>n</i> -C ₉ H ₁₉ -	94	307.5	371.0	63.6
6	4d	H	<i>n</i> -C ₁₀ H ₂₁ -	93	299.5	360.5	61.0
7	4e	CH ₃	<i>n</i> -C ₁₀ H ₂₁ -	96	307.5	379.1	71.6
8	4f	H	<i>n</i> -C ₁₂ H ₂₅ -	93	299.5	367.4	67.9
9 ^b	4g	CH ₃	<i>n</i> -C ₁₂ H ₂₅ -	97	306.5	375.8	69.3
10	4h	H	<i>n</i> -C ₁₄ H ₂₉ -	94	298.0	363.4	65.4
11	4i	CH ₃	<i>n</i> -C ₁₄ H ₂₉ -	95	306.5	368.6	62.1
12	4j	H	<i>n</i> -C ₁₆ H ₃₃ -	95	301.0	363.0	62.0
13	4k	CH ₃	<i>n</i> -C ₁₆ H ₃₃ -	98	306.0	366.9	60.9
14	5a	H	HC≡CCH ₂ -	41	305.5	386.5	81.0
15	5b	CH ₃	HC≡CCH ₂ -	44	306.5	389.5	83.0
16	6	CH ₃		59	309.5	382.5	73.0

^aIn most cases, CH₂Cl₂ is chosen as the solvent for the UV–vis test, and THF is used as the solvent for the fluorescence spectra test. DMSO is used as the solvent only for compounds **3a**, **3b**, and **4a**, due to poor solubility in CH₂Cl₂ and THF. ^bUsing quinine sulfate as a relative standard (0.546),⁴⁴ the fluorescence quantum yield of **3a** (in DMSO) and **4g** (in THF) is 0.23 and 0.20, respectively.

At the same time, due to the potential of triazole-modified derivatives as FCs for nitroaromatic explosives,^{19,23,40} a triazole-modified TBB derivative (e.g., compound **6**, Scheme 3) can be further synthesized by Click reaction,^{19,23,37,38,40} when propargyl bromide is used in N-hydrocarbylation. Finally, 16 TBB compounds (including 15 new compounds) have been prepared (Table 1). The structures of these benzimidazole-type FCs are well characterized by ¹H, ¹³C NMR, ESI-MS, FTIR, UV, and elemental analysis [for details of the corresponding

discussions on the synthesis and characterization, see Supporting Information (SI)].

At the same time, to select appropriate solvent for the following tests of photophysical properties, the solubility of the representative TBB compounds (Table S1, SI) are also preliminarily observed according to the literature,⁴¹ and the results are discussed (see SI).

2.2. Photophysical Properties. 2.2.1. Influences of Different Solvents on Photophysical Properties. To inves-

to investigate whether TBB derivatives **3–6** have the solvatochromism effect,^{42,43} sample solutions of compound **4f** as a model compound in different solvents are prepared first. UV–visible absorptions of samples are shown in Figure 1.

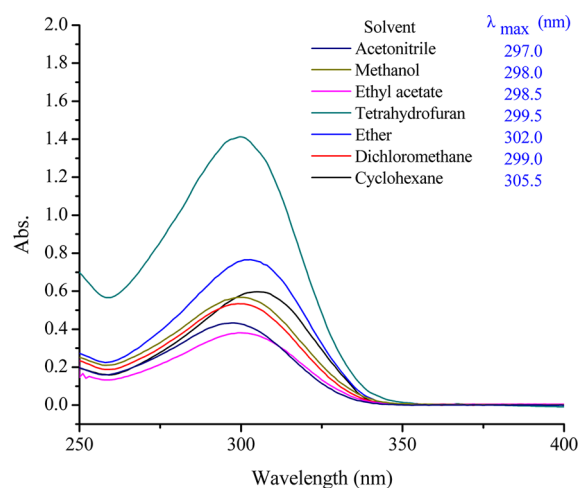


Figure 1. UV–visible spectra of compound **4f** in different solvents.

Obviously, polar solvent has a certain influence on the value of UV absorption maxima (λ_{\max}). Generally, the value of λ_{\max} decreases with the increase in solvent polarity, and the largest difference in λ_{\max} is 8.5 nm for various solvents. The intensity of absorption is not increased with the increase in solvent polarity. When THF is used as the solvent, there is maximum intensity.

Therefore, using THF as solvent, the influences of different concentrations of sample **4f** on the UV–visible absorption are further investigated. As expected, the intensity of absorption is increased with the increase in concentration, but the value of λ_{\max} does not show any change (Figure 2).

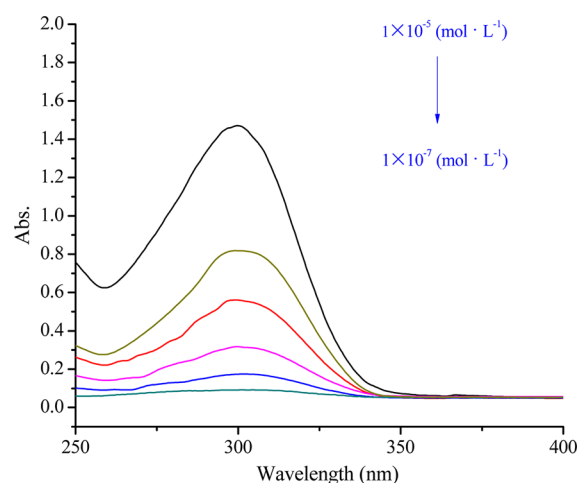


Figure 2. UV–visible spectra of compound **4f** at different concentrations.

According to the fluorescence spectra of typical compound **4f** in different solvents, the fluorescence intensity in THF is the strongest (Figure 3). Thus, THF is chosen as the solvent in most cases for the following fluorescence tests.

2.2.2. Influences of Different Substituents on Photophysical Properties. According to the results obtained above, the UV–visible absorption and fluorescence tests of most

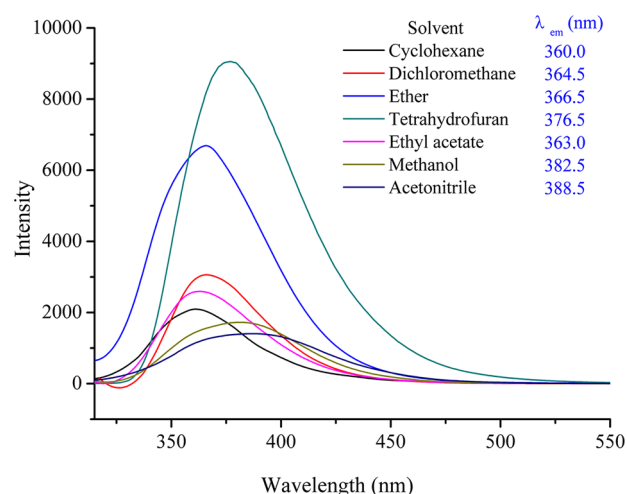


Figure 3. Fluorescence spectra of compound **4f** in different solvents.

compounds are usually carried out in CH_2Cl_2 and THF, respectively. DMSO is used as solvent only for compounds **3** and **4a**, due to the poor solubility in CH_2Cl_2 and THF. The influences of different substituents in compounds **3–6** on photophysical properties are also summarized in Table 1 (the last three columns).

For the same R^1 , the value of λ_{\max} and λ_{em} are relatively smaller (e.g., entries 3 vs 4, 6, 8, 10, Table 1) when the alkyl chain of R^2 is increased. This indicates that a longer alkyl chain may have some influence on the conjugation of the whole molecule somewhat. In fact, the longer alkyl chain R^2 may increase the steric hindrance significantly, actually affecting the planarity of the compounds.

For the same R^2 , the values of λ_{\max} and λ_{em} are usually larger (e.g., entries 1 vs 2, 4 vs 5, 6 vs 7, 8 vs 9, 10 vs 11, 12 vs 13, 14 vs 15, Table 1) when the benzimidazole structure contains a methyl group as substituent. This may be resulted from the fact that the electron-donating methyl favors conjugation in the whole molecule, and the methyl has almost no steric hindrance affecting the planarity of the molecules.

At the same time, as shown in Table 1, the Stokes shifts obtained for all TBB compounds **3–6** are between 60.9 and 83.0 nm, which are appropriate for their use as FCs. Furthermore, according to the literature,⁴⁴ the quantum yields of two typical TBB compounds **3a** and **4g** were tested, respectively, and given as 0.23 and 0.20 (Table 1, entries 1 and 9).

2.3. Detection of Nitroaromatic Explosives in Solution.
2.3.1. Sensing Behaviors of PA toward Different TBB Compounds. On the basis of the above results, the applications of these TBB derivatives as FCs for the detection of PA are further explored. To investigate the influences of different factors in benzimidazole-type FCs, 10 representative compounds are chosen to use in fluorescence titrations with PA (Figure 4, Figure 5, and Figures S49–S56 in SI).

Though the emission band of every compound is basically quenched in the end, the equivalents (equiv) of PA added is different (Table 2). Obviously, when the N–H of compound **3a** is substituted by the saturated alkyl groups R^2 , the quenching becomes better (entries 2–5, 7, 10). Especially, due to the moderate enhancement of the electron-donating effect and solubility effect, the quenching becomes better with the growth of alkyl length when the alkyl chain is less than 14 carbon atoms (entries 2–5). The quenching is reduced when

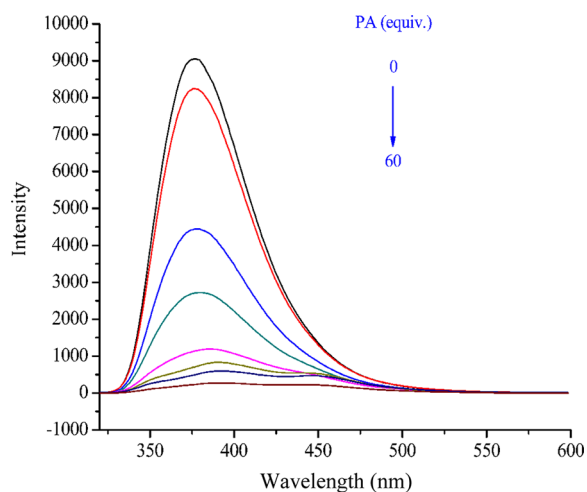


Figure 4. Change in the fluorescence spectra of compound **4f** ($1 \times 10^{-5} \text{ mol}\cdot\text{L}^{-1}$) with the addition of PA in THF solution.

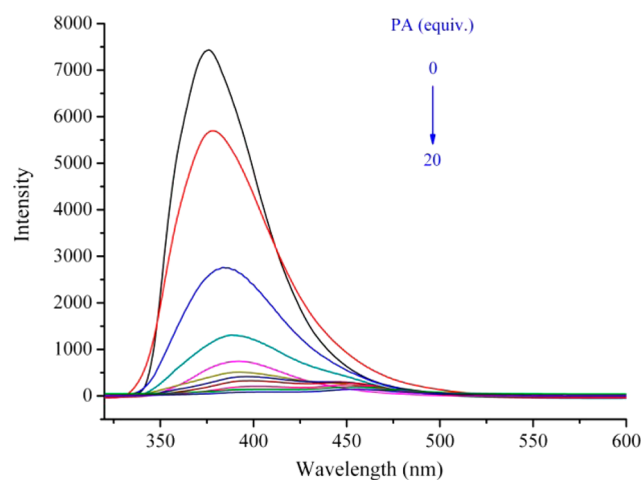


Figure 5. Change in the fluorescence spectra of compound **4g** ($1 \times 10^{-5} \text{ mol}\cdot\text{L}^{-1}$) with the addition of PA in THF solution.

the alkyl chain has 14 carbon atoms (entry 7). Perhaps the steric hindrance of a long alkyl chain is not favorable for the interaction between PA and fluorophore. Thus, the alkyl length has a certain influence on fluorescence quenching, and the influence is not increased with the increase in alkyl chain length, while compound **4f** with 12 carbon atoms is the best among the TBB compounds with $R^1 = \text{H}$ (entry 5).

The fluorescence quenching is also influenced by the saturation of side chain R^2 . A better result is given by the saturated hydrocarbyl (Table 2, entries 2 vs 8). This may be resulted from the stronger electron-donating effect by the alkyl compared to the alkynyl. Similarly, the fluorescence of the chemosensor is more easily quenched by PA (Table 2, entries 6 vs 5, 9 vs 8) when TBB derivatives have a methyl connected to the benzimidazole moiety as an electron-donating group ($R^1 = \text{CH}_3$). According to the experimental results, though the fluorescence quenching of compound **6** is better than that of compound **5a** (Table 2, entries 10 vs 9), the expected result is limited because of the larger steric hindrance from the triazole group (entries 10 vs 6).

Our tests show that the best fluorescence quenching results from a methyl as an electron-donating group and a saturated alkyl chain of suitable length on the benzimidazole ring of TBB

derivatives. Indeed, the fluorescence quenching of compound **4g** ($R^1 = \text{CH}_3$, $R^2 = n\text{-C}_{12}\text{H}_{25}$, Scheme 1) is the best (Table 2, entry 6) and basically achieved by adding 20 equiv of PA (Figure 5). Thus, compound **4g** is selected as a model in the following experiments.

2.3.2. Sensing Behaviors of Various Analytes toward Compound 4g. Using nitromethane (NM) and benzoic acid (BA) as comparative objects,^{10,17,23,45} the fluorescence titrations of compound **4g** with other nitroaromatic explosives, including 2,4,6-trinitrotoluene (TNT), 2,4-dinitrotoluene (DNT), 2,4-dinitrophenol (DNP), 4-nitrotoluene (NT), 4-nitrophenol (NP), 4-nitrobenzaldehyde (NBD), and nitrobenzene (NB), are carried out (Figures S57–S65, see SI). As a comparison with PA, their corresponding data are summarized in Table 3.

For different analytes, the fluorescence quenching is different due to different fluorescence quenching mechanisms. First, for BA, there is a fluorescence enhancement⁴⁵ instead of quenching (Table 3, entry 10). This may be related to the existence of a hydrogen bond^{46–48} or acid–base interaction^{47–49} between the carboxyl and the slightly alkaline benzimidazole derivative **4g**. Second, the fluorescence quenching of nitroalkane NM is far lower than that of the nitroaromatic compounds (Table 3, entries 1–8 vs 9). This implies that the interaction between nitroaromatic compounds and the fluorophore of compound **4g** causes fluorescence quenching more easily. These results are similar to those previously reported.^{10,17,23,45}

Among the nitroaromatics, the quenching becomes better when aromatic analytes have more electron-deficient groups.¹⁹ For example, when there are more nitro groups on the aromatic ring, the fluorescence quenching is more intensive (Table 3, entries 1, 3, 5 and 2, 4, 6). Furthermore, for compounds PA, DNP, and NP with OH groups, the hydrogen bond interaction^{46–48} between them with benzimidazole compound **4g** may be also beneficial to enhance the energy transfer ability to quench the fluorescence of compound **4g**. Thus, PA has the best quenching effect of all (Table 3, entry 1), which also suggests that the benzimidazole-type FC **4g** has a good selectivity for PA.

The fluorescence quenching efficiencies (η) of various analytes toward **4g** are further investigated to confirm this selective recognition. As shown in Figure 6, the fluorescence is basically quenched only by PA. Even for DNP and TNT, their η values are just 56% and 30%, respectively. According to the above results, benzimidazole derivative **4g** is proved as an effective and selective FC for the detection of PA in solution.

2.4. Determination of PA Detection Limit and Stern–Volmer Constant. **2.4.1. Determination of PA Detection Limit (DL).** According to the method in the literature,^{20,22,50} and the datum of C_T (0.005 equiv) from Figure 7, DL for PA can be calculated as follows:

$$\text{CL} = 1 \times 10^{-5} \text{ mol}\cdot\text{L}^{-1}$$

$$\begin{aligned} \text{DL} &= 1 \times 10^{-5} \text{ mol}\cdot\text{L}^{-1} \times 0.005 \text{ equiv} \\ &= 5 \times 10^{-8} \text{ mol}\cdot\text{L}^{-1} \\ &= 50 \text{ ppb} \end{aligned}$$

The result indicates that the benzimidazole-type FC **4g** has better sensitivity than most of the small molecule organic FCs for PA reported previously.^{15,17,19,22}

2.4.2. Calculation of Stern–Volmer Constant (K_{SV}). To further investigate the sensitivity for the detection of PA by **4g**

Table 2. Amount of PA Resulting in 98% Fluorescence Quenching of Different Compounds

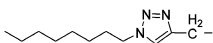
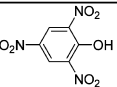
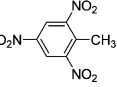
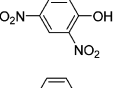
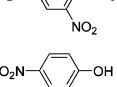
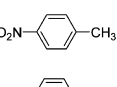
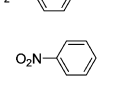
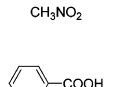
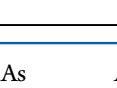
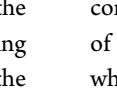
Entry	Compound	R ¹	R ²	Amount (equiv.)
1	3a	H	H	160
2	4a	H	<i>n</i> -C ₃ H ₇ -	140
3	4b	H	<i>n</i> -C ₉ H ₁₉ -	100
4	4d	H	<i>n</i> -C ₁₀ H ₂₁ -	90
5	4f	H	<i>n</i> -C ₁₂ H ₂₅ -	60
6	4g	CH ₃	<i>n</i> -C ₁₂ H ₂₅ -	20
7	4h	H	<i>n</i> -C ₁₄ H ₂₉ -	110
8	5a	H	HC≡CCH ₂ -	170
9	5b	CH ₃	HC≡CCH ₂ -	150
10	6	CH ₃		120

Table 3. Amount of Different Analytes Resulting in 98% Fluorescence Quenching of Compound **4g**

Entry	Compound	Structure	Amount (equiv.)
1	PA		20
2	TNT		280
3	DNP		100
4	DNT		800
5	NP		150
6	NT		1200
7	NBD		600
8	NB		1700
9	NM ^{10, 17, 23}	CH ₃ NO ₂	>8000
10	BA ^{10, 23, 45}		Fluorescence enhancement ⁴⁵

(1×10^{-5} mol·L⁻¹), the Stern–Volmer plot is obtained. As shown in Figure 8, when the concentration of PA is high, the plot bends upward which indicates a superamplified quenching effect.^{19,22,51} The Stern–Volmer plot is linear when the concentration of PA is low.

According to the literature,^{19,22,23} the Stern–Volmer constant (K_{sv}) for PA can be calculated from the above slope of the Stern–Volmer plot, and the value is 1.115×10^5 M⁻¹, which is larger than that reported in the literature.^{14,15,19,22} This means that the benzimidazole-type FC **4g** has sensitivity much

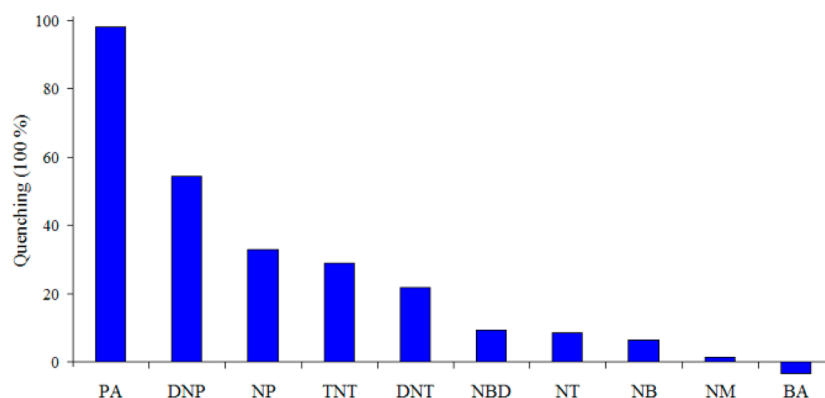


Figure 6. Fluorescence quenching efficiencies toward compound **4g** ($1 \times 10^{-5} \text{ mol} \cdot \text{L}^{-1}$) in THF after the addition of 20 equiv of various analytes.

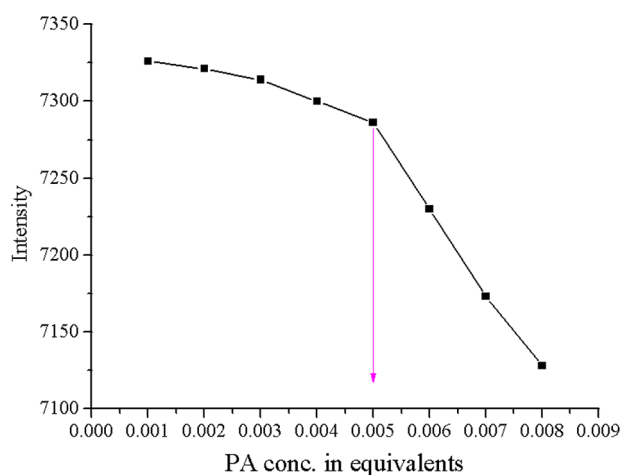


Figure 7. Fluorescence intensity of **4g** at 376 nm as a function of PA concentration.

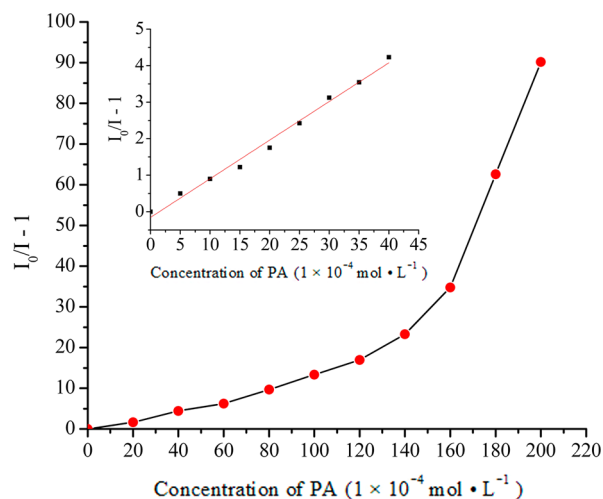


Figure 8. Stern–Volmer plot in response to PA (inset: Stern–Volmer plot obtained at lower concentration of PA).

better than that of the small molecule organic FCs for PA reported previously.^{14,15,19,22}

2.5. Fluorescence Quenching Mechanism. The good selectivity and high sensitivity of FC **4g** for the detection of PA may be related to the fluorescence quenching mechanism. The observed fluorescence quenching for PA is attributed to the energy transfer from photoexcited π -electron rich **4g** to ground-

state electron-deficient PA,^{22,23,25,51,52} which is further confirmed by a large spectral overlap of the emission spectrum of **4g** with the absorption spectrum of PA in the range of 340 to 500 nm (Figure 9).

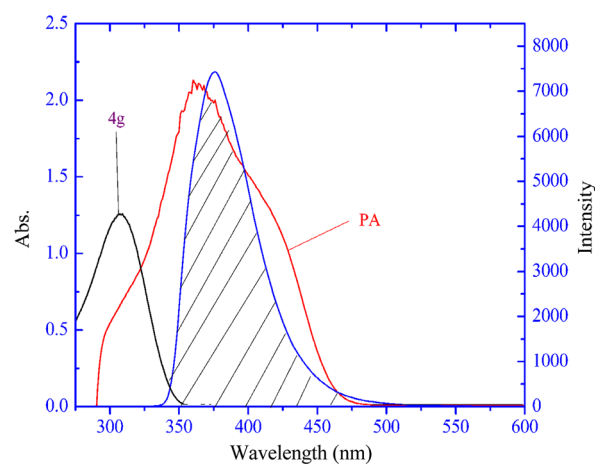


Figure 9. Spectral overlap of the absorption spectra of PA (red line) and **4g** (black line) with the emission spectrum of compound **4g** (blue line).

Notably, the fluorescence titrations of TBB derivative **4g** by addition of 20 equiv of PA at various excitation wavelengths (260–400 nm) are investigated. The η value of PA has no significant change (Figure 10). This means that the decrease in fluorescence intensity of **4g** is not due to masking by PA.^{19,20} The energy transfer mechanism proposed above is proved by the results.

Because there is no spectral overlap between the absorption of TNT and the emission of **4g** (Figure 11), the main quenching mechanism for TNT should be the charge transfer.^{19,22,51} This is confirmed by the result of UV titration of TNT toward compound **4g**. As shown in Figure 12, a level-off tail is formed in the visible region with gradually increasing amounts of TNT (0–120 equiv).

It is well-known that the energy transfer is a long-range process, but the charge transfer is a short-range one.^{22,25,51} PA can interact with the fluorophores of **4g** surrounding it, but TNT only can quench the emission of fluorophores of **4g** that have interaction with it. Thus, compared to TNT, PA is more sensitive to quench the emission of **4g**.

2.6. Visual Detection of PA. **2.6.1. Visual Detection of PA in Solution under UV Light.** Owing to the simple material

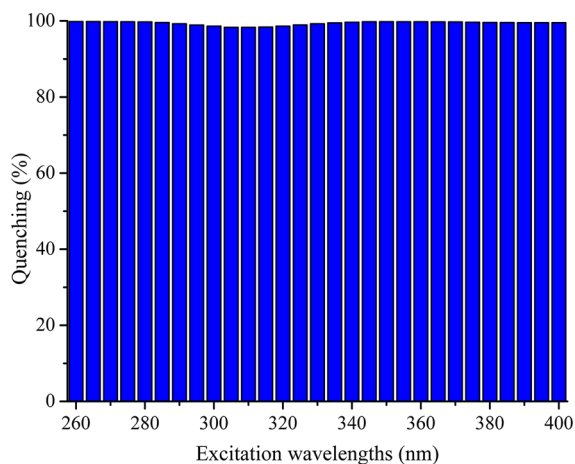


Figure 10. Fluorescence quenching of PA for 4g under different λ_{ex} .

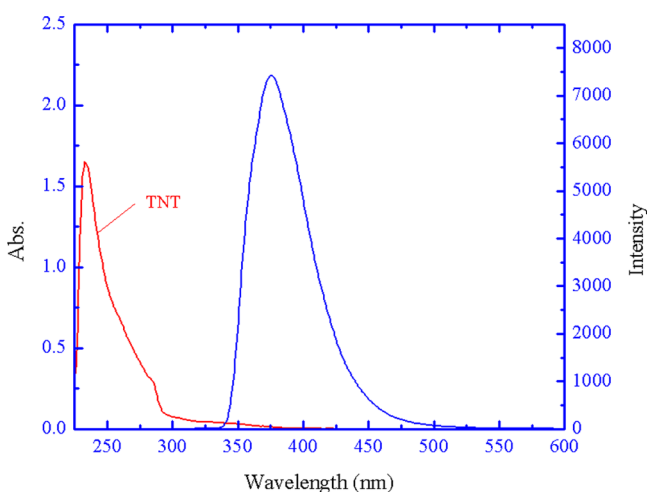


Figure 11. Spectral overlap of the absorption spectrum of TNT (red line) with the emission spectrum of compound 4g (blue line).

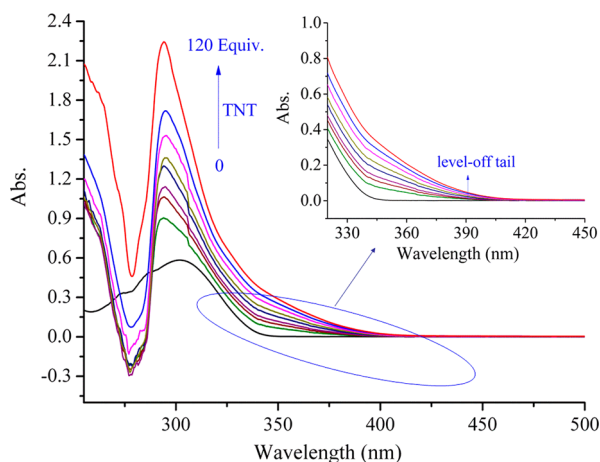


Figure 12. Change in absorption spectra of compound 4g with the addition of TNT in THF (inset: enlarged UV spectra of compound 4g with the addition of TNT in THF in the range of 320–450 nm).

handling, rapid detection, and applicability to practice, the design of visual sensors for the detection of explosives has been a popular field of research^{10,19–23,45,50,52–56}. Among the detection methods, the contact mode approach for testing

nitroaromatics is more important for real time applications to find residual contaminations.^{19–23,53–55}

Therefore, the visual detection of PA in solution under UV light is carried out first. As shown in Figure 13, the color of the

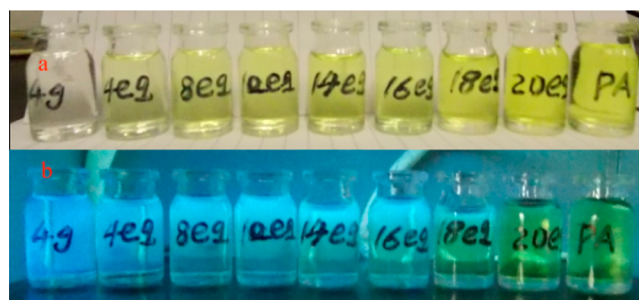


Figure 13. Visual color changes observed upon subjecting a 1×10^{-4} mol·L⁻¹ solution of 4g in THF to an increasing quantity of PA in THF (from left to right, fluorophore 4g, 4–20 equiv of PA) in room light (a) and under UV light (b).

solution of fluorophore 4g and PA in THF changes significantly when the concentration of PA is changed. When 20 equiv of PA is added, the fluorescence is basically quenched, which is consistent with the above results.

2.6.2. Visual Detection of PA in Solid State under UV Light.

PA detection is also carried out in solid state. Compound 4g adsorbed on a thin layer chromatography (TLC) plate shows strong emission (Figure 14a). When a spot of PA solution is adsorbed on compound 4g, there is no emission as observed by the naked eye (Figure 14b).

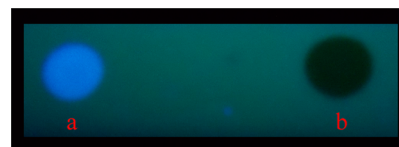


Figure 14. Fluorescence image (under 365 nm UV light) of compound 4g (a) adsorbed on a TLC plate and (b) with a spot of PA solution on compound 4g.

Solution-coated paper strips of 4g are prepared and used to visually detect PA. To investigate the sensitivity of the paper strip for PA, different concentrations of PA (10^{-4} to 10^{-10} mol·L⁻¹) are applied to test strips. As shown in Figure 15, dark spots of different strengths are formed. Therefore, the quenching behavior of 4g is also practically applicable by

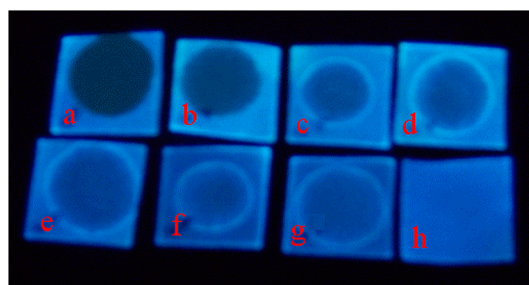


Figure 15. Paper strips of compound 4g for PA detection at different concentrations [(a) 1×10^{-4} mol·L⁻¹, (b) 1×10^{-5} mol·L⁻¹, (c) 1×10^{-6} mol·L⁻¹, (d) 1×10^{-7} mol·L⁻¹, (e) 1×10^{-8} mol·L⁻¹, (f) 1×10^{-9} mol·L⁻¹, (g) 1×10^{-10} mol·L⁻¹, (h) 0] under 365 nm UV light.

varying the concentration of PA even up to the level of 10^{-8} mol·L⁻¹ (Figure 15e). Thus, according to the calculation method in the literature,^{50,55,56} when a 10 μ L volume of 1×10^{-8} mol·L⁻¹ PA solution (22.9 pg PA) is spotted on the paper strips covering an area of about 2 cm², the detection limit (DL) of these **4g** solution-coated paper strips is about 11.45 pg·cm⁻² for PA detection.

For the highly selective detection of PA, there are only a few reports about the DL value of fluorescent paper strips based on small molecule organic FCs without ion-assisted fluorescence enhancement.^{19,20,23} Our obtained DL value can reach the same detection level as that reported previously,¹⁹ and the sensitivity here is better than that reported previously.²³ Therefore, solution-coated paper strips of compound **4g** can be used to visually detect instant trace PA with high sensitivity.

3. CONCLUSION

In summary, a new benzimidazole-type FC for the detection of PA based on the long-range energy transfer mechanism has been successfully designed and synthesized by a simple N-hydrocarbylation of TBB. Among different TBB derivatives, compound **4g** shows good selectivity and high sensitivity to PA, the DL is 50 ppb, and the K_{sv} is 1.115×10^5 M⁻¹. The visual detections are developed, not only in solution, but also in solid state with a thin layer chromatography plate or solution-coated paper strips. Importantly, PA can be detected on these paper strips at the picogram level. Thus, the benzimidazole derivatives can also be viewed as a suitable class of compounds in the development of efficient FCs for the trace detection of PA in solution and contact mode by a significant color change for the first time.

4. EXPERIMENTAL SECTION

4.1. Materials and Equipment. Melting points were uncorrected. Infrared spectra were recorded with an FT-IR spectrometer. ¹H and ¹³C NMR spectra were obtained with a 400 MHz NMR instrument in CDCl₃ (or DMSO-*d*₆) using TMS as an internal standard. Mass spectra (MS) were recorded on a mass spectrometer. Elemental analysis was performed on an elemental analyzer. UV-vis spectra were measured by an ultraviolet absorption detector. The fluorescence spectra were recorded with a spectrophotometer.

All reagents and solvents were commercially available and used as received. Alkyl azide intermediate was prepared according to reported procedures.³⁷

4.2. Synthesis. **4.2.1. Synthesis of Compounds 3.** According to the literature,³² a 100 mL round-bottom flask was charged with 31 mmol of *o*-phenylenediamines **1** and 10 mmol of trimesic acid **2** in the presence of 30 mL of polyphosphoric acid (PPA) as catalyst. The reaction was stirred at 150 °C for 24 h and then stirred at 180 °C for 24 h. After the pH of the resulting mixture was adjusted to 8–9 with 1 mol·L⁻¹ sodium hydroxide (NaOH), a large amount of solid precipitated. After filtration, the crude product was obtained and then further purification by recrystallization with methanol gave **3a,b**.

1,3,5-Tris(1H-benzo[d]imidazol-2-yl)benzene (3a). Yellowish solid 3.455 g, yield 81%, mp >300 °C (>300 °C³²); UV-vis (DMSO) λ_{max} : 316.0 nm; ¹H NMR (400 MHz, DMSO-*d*₆, TMS) δ : 7.20–7.52 (m, 6H), 7.62–7.91 (m, 6H), 9.22 (s, 3H), 13.49 (s, 3H); ¹³C NMR (100 MHz, DMSO-*d*₆, TMS) δ : 112.2, 119.4, 122.4, 123.4, 125.9, 132.3, 135.8, 144.2, 150.8; ESI-MS, *m/z* (%): Calcd for C₂₇H₁₉N₆⁺ ([M + H]⁺): 427.17 (100), found: 427.31 (100).

1,3,5-Tris(6-methyl-1H-benzo[d]imidazol-2-yl)benzene (3b). Yellowish solid 3.842 g, yield 82%, mp >300 °C; UV-vis (DMSO) λ_{max} : 321.0 nm; ¹H NMR (400 MHz, DMSO-*d*₆, TMS) δ : 2.48 (s, 9H), 7.05–7.16 (m, 3H), 7.37–7.65 (m, 6H), 9.04 (s, 3H), 13.11–13.37 (m, 3H); ¹³C NMR (100 MHz, DMSO-*d*₆, TMS) δ : 21.8, 21.9, 111.7, 111.8, 118.9, 119.0, 124.0, 124.8, 125.4, 132.3, 132.8, 136.0, 142.3,

144.6, 150.3; IR (film), ν , cm⁻¹: 3389, 3056, 2977, 2920, 2862, 1578, 1494, 1439, 1343, 860, 803; ESI-MS, *m/z* (%): Calcd for C₃₀H₂₅N₆⁺ ([M + H]⁺): 469.56 (100), found: 469.71 (100). Anal. Calcd for C₃₀H₂₄N₆: C 76.90, H 5.16, N 17.94, found: C 76.95, H 5.01, N 17.89.

4.2.2. Synthesis of Compounds 4. A 50 mL round-bottom flask was charged with 1 mmol of intermediate **3**, 3 mmol of saturated bromoalkanes and 6 mmol of solid NaOH in CH₃CN (10 mL). The reaction was stirred at 80 °C for 12 h. After the solvent was removed, and the residue was dissolved in ethyl acetate. The organic layers were washed with water three times and then dried over anhydrous MgSO₄. The concentration under vacuum gave a crude product, which was purified by column chromatography on silica gel with gradient eluents of petroleum ether and ethyl acetate to afford pure samples **4a,k**.

1,3,5-Tris(1-propyl-1H-benzo[d]imidazol-2-yl)benzene (4a). Yellowish solid 0.337 g, yield 61%, mp 201.1–202.8 °C; UV-vis (CH₂Cl₂) λ_{max} : 301.5 nm; ¹H NMR (400 MHz, CDCl₃, TMS) δ : 0.80 (t, *J* = 8.0 Hz, 9H), 1.76–1.86 (m, 6H), 4.30 (t, *J* = 8.0 Hz, 6H), 7.31–7.35 (m, 6H), 7.41–7.45 (m, 3H), 7.85–7.90 (m, 3H), 8.23 (s, 3H); ¹³C NMR (100 MHz, CDCl₃, TMS) δ : 11.2, 23.2, 46.5, 110.5, 120.0, 123.0, 123.4, 131.4, 131.9, 135.5, 142.6, 151.8; IR (film), ν , cm⁻¹: 3063, 2965, 2925, 2853, 1604, 1507, 1454, 1328, 897, 702, 742; ESI-MS, *m/z* (%): Calcd for C₃₆H₃₇N₆⁺ ([M + H]⁺): 553.31 (100), found: 553.28 (100). Anal. Calcd for C₃₆H₃₆N₆: C 78.23, H 6.57, N 15.21, found: C 78.10, H 6.76, N 15.14.

1,3,5-Tris(1-nonyl-1H-benzo[d]imidazol-2-yl)benzene (4b). Yellowish viscous solid 0.733 g, yield 91%, UV-vis (CH₂Cl₂) λ_{max} : 300.0 nm; ¹H NMR (400 MHz, CDCl₃, TMS) δ : 0.82 (t, *J* = 8.0 Hz, 9H), 1.12–1.30 (m, 36H), 1.84–1.91 (m, 6H), 4.36 (t, *J* = 8.0 Hz, 6H), 7.30–7.36 (m, 6H), 7.44–7.48 (m, 3H), 7.83–7.89 (m, 3H), 8.33 (s, 3H); ¹³C NMR (100 MHz, CDCl₃, TMS) δ : 14.1, 22.6, 26.8, 29.1, 29.2, 29.4, 30.1, 31.8, 45.2, 110.3, 120.2, 122.6, 123.1, 131.1, 132.2, 135.8, 143.2, 151.9; IR (film), ν , cm⁻¹: 3060, 2953, 2924, 2851, 1606, 1500, 1456, 1327, 899, 692, 742; ESI-MS, *m/z* (%): Calcd for C₅₄H₇₃N₆⁺ ([M + H]⁺): 805.59 (100), found: 805.82 (100). Anal. Calcd for C₅₄H₇₂N₆: C 80.55, H 9.01, N 10.44, found: C 80.66, H 8.93, N 10.41.

1,3,5-Tris(6-methyl-1-nonyl-1H-benzo[d]imidazol-2-yl)benzene (4c). Yellowish viscous solid 0.796 g, yield 94%, UV-vis (CH₂Cl₂) λ_{max} : 307.5 nm; ¹H NMR (400 MHz, CDCl₃, TMS) δ : 0.70 (t, *J* = 8.0 Hz, 9H), 1.04–1.14 (m, 36H), 1.73–1.82 (m, 6H), 2.37 (s, 3H), 2.40 (s, 6H), 4.20 (t, *J* = 8.0 Hz, 6H), 6.96–7.06 (m, 3H), 7.10–7.18 (m, 3H), 7.51–7.60 (m, 3H), 8.17 (s, 3H); ¹³C NMR (100 MHz, CDCl₃, TMS) δ : 14.1, 21.5, 21.9, 22.6, 26.8, 29.1, 29.2, 29.4, 29.7, 30.0, 31.8, 45.1, 45.2, 109.8, 110.1, 119.7, 119.9, 124.2, 124.6, 130.7, 130.8, 132.1, 132.2, 133.0, 134.0, 136.1, 141.4, 143.6, 151.5, 151.9; IR (film), ν , cm⁻¹: 3031, 2956, 2922, 2850, 1606, 1502, 1465, 1329, 899, 712, 806; ESI-MS, *m/z* (%): Calcd for C₅₇H₇₉N₆⁺ ([M + H]⁺): 847.64 (100), found: 848.03 (100). Anal. Calcd for C₅₇H₇₈N₆: C 80.80, H 9.28, N 9.92, found: C 80.96, H 9.12, N 9.95.

1,3,5-Tris(1-decyl-1H-benzo[d]imidazol-2-yl)benzene (4d). Yellowish viscous solid 0.788 g, yield 93%, UV-vis (CH₂Cl₂) λ_{max} : 299.5 nm; ¹H NMR (400 MHz, CDCl₃, TMS) δ : 0.87 (t, *J* = 8.0 Hz, 9H), 1.16–1.29 (m, 42H), 1.83–1.91 (m, 6H), 4.36 (t, *J* = 8.0 Hz, 6H), 7.30–7.37 (m, 6H), 7.44–7.48 (m, 3H), 7.82–7.87 (m, 3H), 8.31 (s, 3H); ¹³C NMR (100 MHz, CDCl₃, TMS) δ : 14.1, 22.6, 26.8, 29.1, 29.2, 29.4, 30.1, 31.8, 45.2, 110.3, 120.2, 122.6, 123.1, 131.0, 132.2, 135.9, 143.3, 151.9; IR (film), ν , cm⁻¹: 3064, 2952, 2924, 2853, 1603, 1500, 1454, 1328, 877, 741; ESI-MS, *m/z* (%): Calcd for C₅₇H₇₉N₆⁺ ([M + H]⁺): 847.63 (100), found: 848.13 (100). Anal. Calcd for C₅₇H₇₈N₆: C 80.80, H 9.28, N 9.92, found: C 81.01, H 9.17, N 9.82.

1,3,5-Tris(1-decyl-6-methyl-1H-benzo[d]imidazol-2-yl)benzene (4e). Yellowish viscous solid 0.854 g, yield 96%, UV-vis (CH₂Cl₂) λ_{max} : 307.5 nm; ¹H NMR (400 MHz, CDCl₃, TMS) δ : 0.84 (t, *J* = 8.0 Hz, 9H), 1.14–1.29 (m, 42H), 1.79–1.95 (m, 6H), 2.50 (s, 3H), 2.54 (s, 6H), 4.32 (t, *J* = 8.0 Hz, 6H), 7.13–7.17 (m, 3H), 7.23–7.34 (m, 3H), 7.63–7.73 (m, 3H), 8.28 (s, 3H); ¹³C NMR (100 MHz, CDCl₃, TMS) δ : 14.1, 21.6, 22.0, 22.7, 26.8, 29.2, 29.3, 29.5, 30.0, 31.8, 45.1, 45.2, 109.8, 110.1, 119.7, 120.0, 124.2, 124.6, 130.8, 130.9, 132.1, 132.2, 133.1, 134.0, 136.1, 141.4, 143.6, 151.6, 151.9; IR (film), ν ,

cm⁻¹: 3028, 2926, 2855, 1605, 1465, 1330, 900, 806, 721; ESI-MS, *m/z* (%): Calcd for C₆₀H₈₅N₆⁺ ([M + H]⁺): 889.68 (100), found: 889.80 (100). Anal. Calcd for C₆₀H₈₄N₆: C 81.03, H 9.52, N 9.45, found: C 81.28, H 9.46, N 9.26.

1,3,5-Tris(1-dodecyl-1H-benzo[d]imidazol-2-yl)benzene (4f). Yellowish viscous solid 0.869 g, yield 93%, UV-vis (CH₂Cl₂) λ_{max}: 299.5 nm; ¹H NMR (400 MHz, CDCl₃, TMS) δ: 0.87 (t, *J* = 8.0 Hz, 9H), 1.16–1.29 (m, 54H), 1.83–1.91 (m, 6H), 4.36 (t, *J* = 8.0 Hz, 6H), 7.30–7.37 (m, 6H), 7.44–7.48 (m, 3H), 7.82–7.87 (m, 3H), 8.31 (s, 3H); ¹³C NMR (100 MHz, CDCl₃, TMS) δ: 14.1, 22.7, 26.8, 29.2, 29.3, 29.4, 29.5, 29.6, 30.1, 31.9, 45.2, 110.3, 120.2, 122.7, 123.1, 131.1, 132.1, 135.8, 143.2, 151.9; IR (film), ν, cm⁻¹: 3060, 2926, 2853, 1607, 1499, 1455, 1327, 897, 741; ESI-MS, *m/z* (%): Calcd for C₆₃H₉₁N₆⁺ ([M + H]⁺): 932.44 (100), found: 932.10 (100). Anal. Calcd for C₆₃H₉₀N₆: C 81.24, H 9.74, N 9.02, found: C 81.42, H 9.63, N 8.95.

1,3,5-Tris(1-dodecyl-6-methyl-1H-benzo[d]imidazol-2-yl)benzene (4g). Yellowish viscous solid 0.943 g, yield 97%, UV-vis (CH₂Cl₂) λ_{max}: 306.5 nm; ¹H NMR (400 MHz, CDCl₃, TMS) δ: 0.75 (t, *J* = 8.0 Hz, 9H), 1.04–1.17 (m, 54H), 1.70–1.78 (m, 6H), 2.38 (s, 3H), 2.41 (s, 6H), 4.21 (t, *J* = 8.0 Hz, 6H), 6.97–7.06 (m, 3H), 7.08–7.21 (m, 3H), 7.51–7.61 (m, 3H), 8.17 (s, 3H); ¹³C NMR (100 MHz, CDCl₃, TMS) δ: 14.1, 21.6, 22.0, 22.7, 26.8, 29.2, 29.3, 29.5, 29.6, 30.0, 31.9, 45.1, 45.2, 109.8, 110.1, 119.7, 119.9, 124.2, 124.6, 130.7, 130.8, 132.2, 133.0, 134.0, 136.1, 141.4, 143.6, 151.5, 151.9; IR (film), ν, cm⁻¹: 3028, 2924, 2853, 1606, 1491, 1464, 1328, 899, 806, 721; ESI-MS, *m/z* (%): Calcd for C₆₆H₉₇N₆⁺ ([M + H]⁺): 973.78 (100), found: 974.25 (100). Anal. Calcd for C₆₆H₉₆N₆: C 81.43, H 9.94, N 8.63, found: C 81.40, H 9.81, N 8.79.

1,3,5-Tris(1-tetradecyl-1H-benzo[d]imidazol-2-yl)benzene (4h). Yellowish viscous solid 0.955 g, yield 94%, UV-vis (CH₂Cl₂) λ_{max}: 298.0 nm; ¹H NMR (400 MHz, CDCl₃, TMS) δ: 0.73 (t, *J* = 8.0 Hz, 9H), 1.00–1.15 (m, 66H), 1.66–1.78 (m, 6H), 4.12–4.24 (m, 6H), 7.09–7.16 (m, 6H), 7.22–7.28 (m, 3H), 7.66–7.72 (m, 3H), 8.21 (s, 3H); ¹³C NMR (100 MHz, CDCl₃, TMS) δ: 14.2, 22.7, 26.8, 29.2, 29.3, 29.4, 29.5, 29.6, 29.7, 30.0, 31.9, 45.1, 110.2, 120.2, 122.5, 123.1, 130.9, 132.1, 135.8, 143.2, 151.8; IR (film), ν, cm⁻¹: 3063, 2926, 2851, 1606, 1505, 1455, 1329, 890, 744, 692; ESI-MS, *m/z* (%): Calcd for C₆₉H₁₀₃N₆⁺ ([M + H]⁺): 1015.82 (100), found: 1016.32 (100). Anal. Calcd for C₆₉H₁₀₂N₆: C 81.60, H 10.12, N 8.28, found: C 81.46, H 10.32, N 8.22.

1,3,5-Tris(6-methyl-1-tetradecyl-1H-benzo[d]imidazol-2-yl)benzene (4i). Yellowish viscous solid 1.006 g, yield 95%, UV-vis (CH₂Cl₂) λ_{max}: 306.5 nm; ¹H NMR (400 MHz, CDCl₃, TMS) δ: 0.82 (t, *J* = 8.0 Hz, 9H), 1.08–1.23 (m, 66H), 1.69–1.86 (m, 6H), 2.38 (s, 3H), 2.41 (s, 6H), 4.09–4.31 (m, 6H), 6.96–7.02 (m, 3H), 7.06–7.18 (m, 3H), 7.50–7.65 (m, 3H), 8.25 (s, 3H); ¹³C NMR (100 MHz, CDCl₃, TMS) δ: 14.1, 21.4, 21.8, 22.7, 26.7, 29.2, 29.4, 29.5, 29.6, 29.7, 30.0, 31.9, 44.8, 44.9, 109.6, 109.9, 119.5, 119.8, 124.0, 124.4, 130.5, 131.7, 131.9, 132.7, 134.0, 136.1, 141.4, 143.5, 151.2, 151.6; IR (film), ν, cm⁻¹: 3027, 2924, 2851, 1605, 1465, 1327, 900, 806, 715; ESI-MS, *m/z* (%): Calcd for C₇₂H₁₀₉N₆⁺ ([M + H]⁺): 1057.87 (100), found: 1058.47 (100). Anal. Calcd for C₇₂H₁₁₄N₆: C 81.76, H 10.29, N 7.95, found: C 81.49, H 10.36, N 8.15.

1,3,5-Tris(1-hexadecyl-1H-benzo[d]imidazol-2-yl)benzene (4j). Yellowish viscous solid 1.047 g, yield 95%, UV-vis (CH₂Cl₂) λ_{max}: 301.0 nm; ¹H NMR (400 MHz, CDCl₃, TMS) δ: 0.78 (t, *J* = 8.0 Hz, 9H), 1.05–1.21 (m, 78H), 1.72–1.82 (m, 6H), 4.26 (t, *J* = 8.0 Hz, 6H), 7.16–7.23 (m, 6H), 7.32–7.38 (m, 3H), 7.73–7.78 (m, 3H), 8.22 (s, 3H); ¹³C NMR (100 MHz, CDCl₃, TMS) δ: 14.1, 22.7, 26.8, 29.2, 29.4, 29.5, 29.6, 29.7, 30.1, 32.0, 45.2, 110.3, 120.2, 122.6, 123.1, 131.1, 132.1, 135.8, 143.2, 151.9; IR (film), ν, cm⁻¹: 3063, 2924, 2850, 1606, 1499, 1466, 1454, 1328, 899, 745; ESI-MS, *m/z* (%): Calcd for C₇₅H₁₁₅N₆⁺ ([M + H]⁺): 1099.92 (100), found: 1010.47 (100). Anal. Calcd for C₇₅H₁₁₄N₆: C 81.91, H 10.45, N 7.64, found: C 81.76, H 10.51, N 7.73.

1,3,5-Tris(1-hexadecyl-6-methyl-1H-benzo[d]imidazol-2-yl)benzene (4k). Yellowish viscous solid 1.114 g, yield 98%; UV-vis (CH₂Cl₂) λ_{max}: 306.0 nm; ¹H NMR (400 MHz, CDCl₃, TMS) δ: 0.77 (t, *J* = 8.0 Hz, 9H), 1.05–1.16 (m, 78H), 1.68–1.81 (m, 6H), 2.38 (s, 3H), 2.42 (s, 6H), 4.21 (t, *J* = 8.0 Hz, 6H), 6.98–7.06 (m, 3H), 7.10–

7.21 (m, 3H), 7.49–7.63 (m, 3H), 8.18 (s, 3H); ¹³C NMR (100 MHz, CDCl₃, TMS) δ: 14.1, 21.5, 21.9, 22.7, 26.8, 26.9, 27.7, 29.2, 29.4, 29.5, 29.6, 29.7, 29.8, 30.0, 32.0, 45.0, 45.1, 109.8, 110.1, 119.7, 119.9, 124.2, 124.6, 130.7, 130.8, 132.1, 133.0, 134.0, 136.1, 141.4, 143.6, 151.5, 151.9; IR (film), ν, cm⁻¹: 3029, 2923, 2851, 1604, 1467, 1329, 897, 806, 720; ESI-MS, *m/z* (%): Calcd for C₇₈H₁₂₁N₆⁺ ([M + H]⁺): 1141.97 (100), found: 1142.34 (100). Anal. Calcd for C₇₈H₁₂₀N₆: C 82.05, H 10.59, N 7.36, found: C 81.95, H 10.46, N 7.59.

4.2.3. Synthesis of Compounds 5. A 50 mL round-bottom flask was charged with 1 mmol of intermediate 3, 3 mmol of propargyl bromide, and 6 mmol of NaOH solid in 10 mL of dimethyl sulfoxide (DMSO). The reaction was stirred at 50 °C for 48 h. The resulting mixture was dissolved in ethyl acetate and then washed with water three times. The obtained organic layers were dried over anhydrous MgSO₄ and concentrated under vacuum to give crude product, which was purified by column chromatography on silica gel with gradient eluents of petroleum ether and ethyl acetate to afford pure samples **5a,b**.

1,3,5-Tris(1-(prop-2-yn-1-yl)-1H-benzo[d]imidazol-2-yl)benzene (5a). Yellow solid 0.220 g, yield 41%, mp 268.6–270.6 °C; UV-vis (CH₂Cl₂) λ_{max}: 305.5 nm; ¹H NMR (400 MHz, DMSO-*d*₆, TMS) δ: 3.43 (s, 3H), 5.84 (s, 6H), 7.29–7.38 (m, 6H), 7.69 (d, *J* = 8.0 Hz, 3H), 7.81 (d, *J* = 8.0 Hz, 3H), 8.64 (s, 3H); ¹³C NMR (100 MHz, DMSO-*d*₆, TMS) δ: 34.9, 75.6, 77.2, 110.8, 119.5, 122.5, 125.5, 128.6, 131.7, 133.2, 143.3, 150.3; IR (film), ν, cm⁻¹: 3277, 3053, 2973, 2925, 2137, 1607, 1557, 1457, 1329, 886, 744, 646; ESI-MS, *m/z* (%): Calcd for C₃₆H₂₅N₆⁺ ([M + H]⁺): 541.21 (100), found: 541.42 (100). Anal. Calcd for C₃₆H₂₄N₆: C 79.98, H 4.47, N 15.55, found: C 80.15, H 4.56, N 15.29.

1,3,5-Tris(6-methyl-1-(prop-2-yn-1-yl)-1H-benzo[d]imidazol-2-yl)benzene (5b). Yellow solid 0.256 g, yield 44%, mp 273.4–275.1 °C; UV-vis (CH₂Cl₂) λ_{max}: 306.5 nm; ¹H NMR (400 MHz, DMSO-*d*₆, TMS) δ: 2.49 (s, 3H), 2.53 (s, 6H), 3.51 (s, 2H), 3.56 (s, 1H), 5.33 (s, 6H), 7.19 (d, *J* = 8.0 Hz, 2H), 7.24 (d, *J* = 8.0 Hz, 1H), 7.58 (s, 2H), 7.61 (s, 1H), 7.66 (d, *J* = 8.0 Hz, 1H), 7.70 (d, *J* = 8.0 Hz, 2H), 8.51 (s, 2H), 8.55 (s, 1H); ¹³C NMR (100 MHz, DMSO-*d*₆, TMS) δ: 21.2, 21.5, 34.4, 34.5, 76.5, 78.3, 78.4, 110.6, 110.7, 119.2, 119.3, 124.3, 124.7, 130.3, 130.4, 131.2, 131.9, 132.8, 133.7, 135.8, 140.7, 142.9, 150.6, 151.0; IR (film), ν, cm⁻¹: 3286, 3030, 2920, 2858, 2121, 1607, 1500, 1447, 1325, 897, 804, 648; ESI-MS, *m/z* (%): Calcd for C₃₉H₃₁N₆⁺ ([M + H]⁺): 583.70 (100), found: 583.59 (100). Anal. Calcd for C₃₉H₃₀N₆: C 80.39, H 5.19, N 14.42, found: C 80.18, H 5.36, N 14.46.

4.2.4. Synthesis of Compound 6. According to the literature,^{19,23,37,38} a 50 mL round-bottom flask was charged with 1 mmol of intermediate 5, 4 mmol of alkyl azide intermediate, 10% mmol Cu, and 5% mmol CuSO₄ in DMSO (5 mL). The reaction was stirred at 50 °C for 48 h. The resulting mixture was extracted with ethyl acetate (10 mL × 3) and then washed with water three times. The organic layers were dried over anhydrous MgSO₄ and concentrated under vacuum to give crude product, which was purified by column chromatography on silica gel with gradient eluents of petroleum ether and ethyl acetate to afford pure sample **6**.

1,3,5-Tris(5-methyl-1-((1-octyl-1H-1,2,3-triazol-4-yl)methyl)-1H-benzo[d]imidazol-2-yl)benzene (6). Yellow solid 0.616 g, yield 59%, mp 121.1–122.5 °C; UV-vis (CH₂Cl₂) λ_{max}: 309.5 nm; ¹H NMR (400 MHz, DMSO-*d*₆, TMS) δ: 0.79 (t, *J* = 8.0 Hz, 9H), 1.07–1.23 (m, 30H), 1.62–1.72 (m, 6H), 2.44 (s, 3H), 2.46 (s, 6H), 4.24 (t, *J* = 8.0 Hz, 6H), 5.64 (s, 4H), 5.67 (s, 2H), 7.09–7.16 (m, 3H), 7.53 (s, 3H), 7.62 (d, *J* = 8.0 Hz, 3H), 8.24 (s, 3H), 8.57 (s, 3H); ¹³C NMR (100 MHz, DMSO-*d*₆, TMS) δ: 13.8, 21.1, 22.0, 25.7, 28.2, 28.4, 29.6, 31.1, 49.4, 54.0, 111.0, 118.9, 123.6, 123.9, 125.5, 131.5, 132.3, 133.9, 136.0, 142.3, 151.3; IR (film), ν, cm⁻¹: 3139, 3057, 2955, 2925, 2851, 1606, 1544, 1509, 1459, 1327, 873, 803; ESI-MS, *m/z* (%): Calcd for C₆₃H₈₂N₁₅⁺ ([M + H]⁺): 1048.69 (100), found: 1048.89 (100). Anal. Calcd for C₆₃H₈₁N₁₅: C 72.17, H 7.79, N 20.04, found: C 72.40, H 7.90, N 19.99.

4.3. Application. **4.3.1. Fluorescence Quenching Titration in Organic Media.** According to the literature,^{16,22–24,45} fluorescence quenching titrations in organic solvents were carried out by placing 2

mL of 1×10^{-5} mol·L⁻¹ solution of benzimidazole derivatives (e.g., **4g**) in a quartz cuvette of 1 cm width. Then, a tetrahydrofuran (THF) solution of analytes (e.g., PA) was added in an incremental fashion. For each addition, at least three fluorescence spectra were recorded repeatedly at 298 K to obtain a concordant value. For all measurements, every benzimidazole-type compound was excited at its λ_{ex} (e.g., for **4g**, $\lambda_{\text{ex}} = 307$ nm) and their emissions were monitored within the suitable region (e.g., for **4g**, 317–600 nm) while keeping 2 nm slit width for both source and detector.

The fluorescence quenching efficiency (η) for each analyte was calculated by the following equation:

$$\eta = (I_0 - I)/I_0 \times 100\%$$

where I_0 and I are the fluorescence intensities in the absence and presence of analyte, respectively.

4.3.2. Determination of PA Detection Limit. According to the literature,^{20,22,50} the fluorescence titration of compound **4g** in THF solution with PA was carried out by adding aliquots of PA solution. Then, the fluorescence intensity as a function of the added PA amount was plotted. From this graph, when there was a sharp change in the fluorescence intensity, the corresponding concentration could be obtained as C_T . Multiplying C_T with C_L (the concentration of compound **4g**) as in the following equation gave the detection limit (DL):

$$DL = C_L \times C_T$$

4.3.3. Calculation of Stern–Volmer Constant. According to the literature,^{19,22,23} the sensitivity of chemosensor **4g** toward PA was estimated from the Stern–Volmer constant (K_{sv}). The Stern–Volmer plot was plotted as a function of the PA concentration ($[Q]$) as in the following equation:

$$I_0/I = 1 + K_{\text{sv}} \times [Q]$$

Thus, K_{sv} can be calculated from the slope of the Stern–Volmer plot.

4.3.4. Visual Detection of PA in Solution under UV Light. According to the literature,⁴⁵ after a 1×10^{-4} mol·L⁻¹ THF solution of **4g** was equally placed in identical glass bottles, PA of different amounts (4–20 equiv) was added, respectively. Under UV light at 365 nm, the results were observed, and the photos were obtained.

4.3.5. Visual Detection of PA on a Thin Layer Chromatography (TLC) Plate under UV Light. According to the literature,^{22,23,53,54} after dropping a THF solution of **4g** (1×10^{-4} mol·L⁻¹) onto a spot at both ends of a TLC plate, respectively, drying the plate under vacuum makes **4g** supported. Then, onto one of the spots was dropped PA solution, and the plate was dried under vacuum. Under UV light at 365 nm, the results were observed, and the photos were obtained.

4.3.6. Visual Detection of PA on Solution-Coated Paper Strips under UV Light. According to the literature,^{10,50,55–57} a piece of Whatman filter paper (1.5×1.5 cm²) was immersed in a THF solution of **4g** (1×10^{-4} mol·L⁻¹) for 10 min. Then, the filter paper was removed from the solution and dried under vacuum at 50 °C for 24 h. Under irradiation with a UV lamp at 365 nm, this filter paper emitted strong fluorescence. To demonstrate its application as a fluorescence paper sensor for PA detection, THF solutions of PA at different concentrations (10^{-4} to 10^{-10} mol·L⁻¹) were spotted onto test strips at the desired concentration level using a micropipette. After drying the strips under vacuum, the results were observed with 365 nm UV light, and the photos were obtained.

■ ASSOCIATED CONTENT

📄 Supporting Information

Some detailed discussions of the synthesis, characterization, and solubility testing of compounds **3–6**; ¹H and ¹³C NMR and mass spectra of all TBB derivatives **3–6** and other fluorescence spectra of different titrations. This material is available free of charge via the Internet at <http://pubs.acs.org>.

■ AUTHOR INFORMATION

Corresponding Authors

*E-mail: wangzy@scnu.edu.cn. Tel: 8620-39310258.

*E-mail: xiaoyun.chen@oc.rwth-aachen.de.

Author Contributions

[§]J.-F. Xiong and J.-X. Li contributed equally to this work.

Notes

The authors declare no competing financial interest.

■ ACKNOWLEDGMENTS

We are grateful to the NNSFC (no. 20772035), the third Talents Special Funds of Guangdong Higher Education (no. Guangdong-Finance-Education [2011]431), and the NSF of Guangdong Province (no. S2011010001556) for financial support. We also thank Prof. and Dr. Ling-Yun Wang for her helpful discussion and support in partial test experiments.

■ REFERENCES

- (1) Bhattacharjee, Y. *Science* **2008**, *320*, 1416–1417.
- (2) Germain, M. E.; Knapp, M. J. *Chem. Soc. Rev.* **2009**, *38*, 2543–2555.
- (3) Zhang, K.; Zhou, H.; Mei, Q.; Wang, S.; Guan, G.; Liu, R.; Zhang, J.; Zhang, Z. *J. Am. Chem. Soc.* **2011**, *133*, 8424–8427.
- (4) Liao, Y. Z.; Strong, V.; Wang, Y.; Li, X. G.; Wang, X.; Kaner, R. B. *Adv. Funct. Mater.* **2012**, *22*, 726–735.
- (5) Nagarkar, S. S.; Joarder, B.; Chaudhari, A. K.; Mukherjee, S.; Ghosh, S. K. *Angew. Chem., Int. Ed.* **2013**, *52*, 2881–2885.
- (6) Bejoymohandas, K. S.; George, T. M.; Bhattacharya, S.; Natarajan, S.; Reddy, M. L. P. *J. Mater. Chem. C* **2014**, *2*, 515–523.
- (7) Tian, D.; Li, Y.; Chen, R. Y.; Chang, Z.; Wang, G. Y.; Bu, X. H. *J. Mater. Chem. A* **2014**, *2*, 1465–1470.
- (8) Liu, T. H.; Ding, L. P.; He, G.; Yang, Y.; Wang, W. L.; Fang, Y. *ACS Appl. Mater. Interfaces* **2011**, *3*, 1245–1253.
- (9) Ma, Y. X.; Li, H.; Peng, S.; Wang, L. Y. *Anal. Chem.* **2012**, *84*, 8415–8421.
- (10) Bhalla, V.; Kaur, S.; Vij, V.; Kumar, M. *Inorg. Chem.* **2013**, *52*, 4860–4865.
- (11) Li, X. G.; Liao, Y. Z.; Huang, M. R.; Strong, V.; Kaner, R. B. *Chem. Sci.* **2013**, *4*, 1970–1978.
- (12) Xu, Y. Q.; Li, B. H.; Li, W. W.; Zhao, J.; Sun, S. G.; Pang, Y. *Chem. Commun.* **2013**, *49*, 4764–4766.
- (13) Kumar, S.; Venkatramaiah, N.; Patil, S. J. *Phys. Chem. C* **2013**, *117*, 7236–7245.
- (14) Venkatramaiah, N.; Kumar, S.; Patil, S. *Chem. Commun.* **2012**, *48*, 5007–5009.
- (15) Kumar, M.; Reja, S. I.; Bhalla, V. *Org. Lett.* **2012**, *14*, 6084–6087.
- (16) Samanta, D.; Mukherjee, P. S. *Dalton Trans.* **2013**, *42*, 16784–16795.
- (17) Zhou, X. H.; Li, L.; Li, H. H.; Li, A.; Yang, T.; Huang, W. *Dalton Trans.* **2013**, *42*, 12403–12409.
- (18) Li, H. M.; Zhu, Y. X.; Zhang, J. Y.; Chi, Z. G.; Chen, L. P.; Su, C. Y. *RSC Adv.* **2013**, *3*, 16340–16344.
- (19) Bhalla, V.; Gupta, A.; Kumar, M.; Rao, D. S.; Prasad, S. K. *ACS Appl. Mater. Interfaces* **2013**, *5*, 672–679.
- (20) Vij, V.; Bhalla, V.; Kumar, M. *ACS Appl. Mater. Interfaces* **2013**, *5*, 5373–5380.
- (21) Dey, N.; Samanta, S. K.; Bhattacharya, S. *ACS Appl. Mater. Interfaces* **2013**, *5*, 8394–8400.
- (22) Bhalla, V.; Gupta, A.; Kumar, M. *Org. Lett.* **2012**, *14*, 3112–3115.
- (23) Bhalla, V.; Arora, H.; Singh, H.; Kumar, M. *Dalton Trans.* **2013**, *42*, 969–974.
- (24) Roy, B.; Bar, A. K.; Gole, B.; Mukherjee, P. S. *J. Org. Chem.* **2013**, *78*, 1306–1310.

- (25) Valeur, B. *Molecular fluorescence: Principle and applications*; Wiley-VCH: Weinheim, 2002.
- (26) Mao, Z. Z.; Wang, Z. Y.; Li, J. N.; Song, X. M.; Luo, Y. F. *Synth. Commun.* **2010**, *40*, 1963–1977.
- (27) Frei, R.; Breitbach, A. S.; Blackwell, H. E. *Angew. Chem., Int. Ed.* **2012**, *51*, 5226–5229.
- (28) Narasimhan, B.; Sharma, D.; Kumar, P. *Med. Chem. Res.* **2012**, *21*, 269–283.
- (29) Peng, P.; Xiong, J. F.; Mo, G. Z.; Zheng, J. L.; Chen, R. H.; Chen, X. Y.; Wang, Z. Y. *Amino Acids* **2014**, *46*, 2427–2433.
- (30) Wiggins, K. M.; Kerr, R. L.; Chen, Z.; Bielawski, C. W. *J. Mater. Chem.* **2010**, *20*, 5709–5714.
- (31) Muth, M.; Rasco-Orozco, M.; Thelakkat, M. *Adv. Funct. Mater.* **2011**, *21*, 4510–4518.
- (32) Xiong, J. F.; Luo, S. H.; Huo, J. P.; Liu, J. Y.; Chen, S. X.; Wang, Z. Y. *J. Org. Chem.* **2014**, *79*, 8366–8373.
- (33) Xiong, J. F.; Luo, S. H.; Wang, Q. F.; Wang, Z. Y.; Qi, J. *Des. Monomers Polym.* **2013**, *16*, 389–397.
- (34) Zhu, K.; Vukotic, V. N.; Loeb, S. J. *Angew. Chem., Int. Ed.* **2012**, *51*, 2168–2172.
- (35) He, Q. T.; Li, X. P.; Liu, Y.; Yu, Z. Q.; Wang, W.; Su, C. Y. *Angew. Chem., Int. Ed.* **2009**, *48*, 6156–6159.
- (36) Guo, Z.; Song, N. R.; Moon, J. H.; Kim, M.; Jun, E. J.; Choi, J.; Lee, J. Y.; Bielawski, C. W.; Sessler, J. L.; Yoon, J. *J. Am. Chem. Soc.* **2012**, *134*, 17846–17849.
- (37) Tan, Y. H.; Li, J. X.; Xue, F. L.; Qi, J.; Wang, Z. Y. *Tetrahedron* **2012**, *68*, 2827–2843.
- (38) Huo, J. P.; Luo, J. C.; Wu, W.; Xiong, J. F.; Mo, G. Z.; Wang, Z. Y. *Ind. Eng. Chem. Res.* **2013**, *52*, 11850–11857.
- (39) Chen, R. H.; Xiong, J. F.; Peng, P.; Mo, G. Z.; Tang, X. S.; Wang, Z. Y.; Wang, X. F. *Asian J. Chem.* **2014**, *26*, 926–932.
- (40) Bhalla, V.; Singh, H.; Kumar, M.; Prasad, S. K. *Langmuir* **2011**, *27*, 15275–15281.
- (41) Wang, B.; Liu, C. J.; Wang, J. D.; Lei, Z. K.; Hu, D. L. *Chem. J. Chin. Univ.* **2012**, *33*, 76–81.
- (42) Tanabe, K.; Suzui, Y.; Hasegawa, M.; Kato, T. *J. Am. Chem. Soc.* **2012**, *134*, 5652–5661.
- (43) Ahipaa, T. N.; Kumar, V.; Adhikari, A. V. *Liq. Cryst.* **2013**, *40*, 31–38.
- (44) Vieira, A. A.; Gallardo, H.; Barberá, J.; Romero, P.; Serrano, J. L.; Sierra, T. *J. Mater. Chem.* **2011**, *21*, 5916–5922.
- (45) Shanmugaraju, S.; Joshi, S. A.; Mukherjee, P. S. *J. Mater. Chem.* **2011**, *21*, 9130–9138.
- (46) Ueki, T.; Watanabe, M. *Macromolecules* **2008**, *41*, 3739–3749.
- (47) Iwan, A.; Kaczmarczyk, B.; Jarzabek, B.; Jurusik, J.; Domanski, M.; Michalak, M. *J. Phys. Chem. A* **2008**, *112*, 7556–7566.
- (48) Zuo, Z. C.; Fu, Y. Z.; Manthiram, A. *Polymers* **2012**, *4*, 1627–1644.
- (49) Fu, Y. Z.; Manthiram, A. *J. Electrochem. Soc.* **2007**, *154*, B8–B12.
- (50) Pramanik, S.; Bhalla, V.; Kumar, M. *Anal. Chim. Acta* **2013**, *793*, 99–106.
- (51) Wang, J.; Mei, J.; Yuan, W. Z.; Liu, P.; Qin, A. J.; Sun, J. Z.; Ma, Y. G.; Tang, B. Z. *J. Mater. Chem.* **2011**, *21*, 4056–4059.
- (52) Li, D. D.; Liu, J. Z.; Kwok, R. T.; Liang, Z. Q.; Tang, B. Z.; Yu, J. H. *Chem. Commun.* **2012**, *48*, 7167–7169.
- (53) Venkatramaiah, N.; Kumar, S.; Patil, S. *Chem.—Eur. J.* **2012**, *18*, 14745–14751.
- (54) Martinez, H. P.; Grant, C. D.; Reynolds, J. G.; Troglor, W. C. *J. Mater. Chem.* **2012**, *22*, 2908–2914.
- (55) Kartha, K. K.; Babu, S. S.; Srinivasan, S.; Ajayaghosh, A. *J. Am. Chem. Soc.* **2012**, *134*, 4834–4841.
- (56) Bhalla, V.; Pramanik, S.; Kumar, M. *Chem. Commun.* **2013**, *49*, 895–897.
- (57) Kumar, M.; Vij, V.; Bhalla, V. *Langmuir* **2012**, *28*, 12417–12421.